

Theory analysis of wavelength dependence of laser-induced phase explosion of silicon

Quanming Lu,^{1,2} Samuel S. Mao,^{1,3} Xianglei Mao,¹ and Richard E. Russo^{1,a)}

¹Lawrence Berkeley National Laboratory, Berkeley, California 94720, USA

²School of Earth and Space Sciences, University of Science and Technology of China, Hefei 230026, China

³Department of Mechanical Engineering, University of California, Berkeley, California 94720, USA

(Received 14 May 2008; accepted 18 July 2008; published online 21 October 2008)

Wavelength dependence of laser ablation of silicon was investigated with nanosecond ultraviolet, visible, and infrared laser pulses in the irradiance range from 3×10^{10} to $1 \times 10^{12} \text{ W/cm}^2$. For 266 and 532 nm laser pulses, the depth of laser-produced crater shows a dramatic increase at a laser irradiance threshold of approximately 2×10^{10} and $4 \times 10^{11} \text{ W/cm}^2$ respectively, above which, large micron-sized particulates were observed to eject from the target about 300–400 ns after the laser pulse. In contrast, for 1064 nm pulse, this dramatic increase was not observed. The underlying mechanism for the observed threshold phenomenon is presented in this study, which can be attributed to the thermal diffusion and subsequent explosive boiling after the completion of the interaction between the nanosecond laser pulse and silicon. Based on our delayed phase explosive model, the ablation depths were calculated for different wavelengths and compared to experimental results. Plasma shielding during laser irradiation was included in the model, which plays a key role to the coupling of laser energy to the irradiated material. © 2008 American Institute of Physics.

[DOI: [10.1063/1.2978369](https://doi.org/10.1063/1.2978369)]

I. INTRODUCTION

During the past few years, interactions of laser pulses and materials have attracted considerable attention due to their applications in a number of areas, such as deposition of thin films and laser-based chemical analysis.^{1,2} One key parameter in characterizing how well is the coupling of laser energy with a solid is the relationship between the ablation depth versus the laser irradiance. The removal of mass from the target by a laser pulse can occur by both thermal and nonthermal mechanisms. For nonthermal mechanism, it is suggested that the incident laser radiation can induce a large population of electrons to a highly excited nonequilibrium state near the surface, which leads to bond breaking of the target material and subsequently causes ions ejected from the target surface.³ For the thermal mechanism, the excited electrons transfer absorbed energy to ions by the electron-phonon relaxation process, while the heat is conducted into the solid lattice. The conducted heat can melt the sample and bring its local temperature far beyond the boiling temperature.⁴ For nanosecond laser interaction with solids, thermal mechanism appears to be the dominant mechanism.⁵

When the laser irradiance exceeds 10^9 W/cm^2 for a nanosecond laser pulse, the temperature near the surface of a solid target can exceed the boiling point, thus a superheated liquid layer is formed.⁶ It was suggested that explosive boiling takes place where homogeneous vapor bubble nucleation occurs when the target material reaches $\sim 0.90T_{\text{tc}}$ (T_{tc} is the thermodynamic critical temperature). As a consequence, the target material makes an abrupt transformation from superheated liquid into a mixture of liquid droplets and vapor,

which are then ejected from the target.^{7,8} Laser ablation from single-crystal silicon with laser irradiance 10^9 – 10^{11} W/cm^2 (single pulse) was studied^{9,10} in an experiment using a Nd:YAG (yttrium aluminum garnet) laser with 266 nm wavelength and 3 ns pulse duration. The results showed that the ablation depth increased dramatically at the laser irradiance threshold of approximately $2 \times 10^{10} \text{ W/cm}^2$; above this threshold, large particulates were ejected from the target surface about 300–400 ns after laser interaction. A laser-induced transparent layer when the temperature approached the critical temperature was speculated to result in the abrupt increase in the ablation depth at the threshold.¹⁰ However, experiments were unable to verify such a transparent layer during pulsed laser ablation of solids.

We developed an alternative theory based on delayed phase explosion model¹¹ that was able to interpret the experimental observation of UV laser ablation. In this article, we extend our theoretical analysis by examining laser wavelength dependence of experimentally observed threshold behavior of phase explosion. In the following, we first present an overview of experimental results of ablation depth as a function of laser irradiance.

II. RESULTS FROM EXPERIMENTS

In previous experiments, a Nd:YAG laser with 266, 532, and 1064 nm wavelengths and 3 ns pulse duration is focused to $\sim 35 \mu\text{m}$ diameter spot on a single-crystal silicon target; the laser irradiance varies from 3×10^9 to $1.2 \times 10^{12} \text{ W/cm}^2$. A second Nd-YAG laser of pulse duration 35 ps was used as a probe beam to record shadowgraph images of mass ejection from the laser-irradiated silicon surface. This 532 nm wavelength probe beam was aligned parallel to the silicon surface and perpendicular to the ablation laser

^{a)}Author to whom correspondence should be addressed. Electronic mail: rerusso@lbl.gov.

Report Documentation Page			Form Approved OMB No. 0704-0188		
<p>Public reporting burden for the collection of information is estimated to average 1 hour per response, including the time for reviewing instructions, searching existing data sources, gathering and maintaining the data needed, and completing and reviewing the collection of information. Send comments regarding this burden estimate or any other aspect of this collection of information, including suggestions for reducing this burden, to Washington Headquarters Services, Directorate for Information Operations and Reports, 1215 Jefferson Davis Highway, Suite 1204, Arlington VA 22202-4302. Respondents should be aware that notwithstanding any other provision of law, no person shall be subject to a penalty for failing to comply with a collection of information if it does not display a currently valid OMB control number.</p>					
1. REPORT DATE 2008	2. REPORT TYPE	3. DATES COVERED			
4. TITLE AND SUBTITLE Theory analysis of wavelength dependence of laser-induced phase explosion of silicon			5a. CONTRACT NUMBER W911NF-06-1-0446	5b. GRANT NUMBER	
			5c. PROGRAM ELEMENT NUMBER		
6. AUTHOR(S)			5d. PROJECT NUMBER	5e. TASK NUMBER	
			5f. WORK UNIT NUMBER		
7. PERFORMING ORGANIZATION NAME(S) AND ADDRESS(ES) Lawrence Berkeley National Laboratory, Berkeley, CA, 94720			8. PERFORMING ORGANIZATION REPORT NUMBER		
9. SPONSORING/MONITORING AGENCY NAME(S) AND ADDRESS(ES)			10. SPONSOR/MONITOR'S ACRONYM(S)		
			11. SPONSOR/MONITOR'S REPORT NUMBER(S)		
12. DISTRIBUTION/AVAILABILITY STATEMENT Approved for public release; distribution unlimited.					
13. SUPPLEMENTARY NOTES					
14. ABSTRACT					
15. SUBJECT TERMS					
16. SECURITY CLASSIFICATION OF: a. REPORT b. ABSTRACT c. THIS PAGE unclassified unclassified unclassified			17. LIMITATION OF ABSTRACT	18. NUMBER OF PAGES 8	19a. NAME OF RESPONSIBLE PERSON

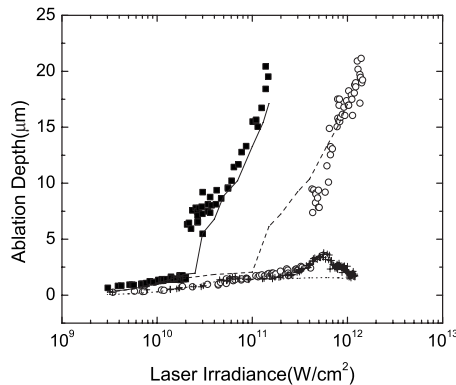


FIG. 1. Comparison of measured ablation depths with the computational data (■: measured ablation depth for 266 nm wavelength, ○: measured ablation depth for 532 nm wavelength, +: measured ablation depth for 1064 wavelength. The solid line for the computational ablation depth for 266 nm wavelength, the dash line for the computational ablation depth for 532 nm wavelength, and the dot line for computational ablation depth for 1064 nm wavelength.).

beam. The time delay of the probe laser pulse with respect to the ablation pulse was controlled by a four-channel digital delay/pulse generator and monitored using a digital oscilloscope. The depth of the crater was measured with a white light interferometric microscope (Zygo model NewView 200). By measuring ablation depth versus laser irradiance at different wavelengths (Fig. 1), it was realized that the ablation depth increases dramatically at the laser irradiance threshold of about 2×10^{10} and 4×10^{11} W/cm² for 266 and 532 nm wavelength laser pulses, respectively. For the 266 nm wavelength, the ablation depth increases gradually from 0.6 to 1.5 μm as the laser irradiance increases from 3.0×10^9 to 2.0×10^{10} W/cm², then it abruptly increases from 1.5 to 6.3 μm, and reaches 20 μm at 1.5×10^{11} W/cm². For 532 nm wavelength, the ablation depth increases from 0.26 to 2.5 μm as laser irradiance is increased from 3.4×10^9 to 4.0×10^{11} W/cm², and beyond a threshold, the ablation depth changes sharply from 2.5 to 7.4 μm. For 1064 nm wavelength laser pulse, however, such a dramatic increase does not exist, the ablation depth increases gradually from 0.24 to 3.8 μm when laser irradiance varied from 3.4×10^9 to 5.6×10^{11} W/cm², then gradually decreases to 1.7 μm at 1.2×10^{12} W/cm². A shock wave was observed to last about several tens of nanoseconds after the laser pulse, which was formed due to the pressure difference between a dense plasma and the ambient.^{12,13} For 266 and 532 nm wavelength laser pulses, when the laser irradiance exceeds the respective threshold, there are large particulates ejected from the target surface about 300–400 ns after the laser irradiation, while for 1064 nm wavelength, there were no such large particulates.

III. ANALYSIS

There are two basic types of thermal processes for laser ablation.⁸ The first is normal vaporization, which occurs at extreme outer surface for any laser irradiance and pulse duration.^{14,15} The vaporization flux is governed by the Hertz-

Knudsen equations, and the velocity of surface recession can be given if multiplied by m/ρ (m being the particle mass and ρ the target mass density):

$$\left. \frac{\partial x}{\partial t} \right|_{x=0} = \beta(p_b - p_{\text{amb}}) \frac{m}{\rho} (2\pi mk_B T)^{-1/2} \times \exp\left[\frac{L_{\text{ev}} m}{k_B} \left(\frac{1}{T_b} - \frac{1}{T}\right)\right] \text{ cm/s.} \quad (1)$$

Here, β is the vaporization coefficient,¹⁶ p_b is the boiling pressure (~ 0.1 MPa), p_{amb} is the ambient vapor pressure, T_b is the corresponding boiling temperature, k_B is the Boltzmann constant, and L_{ev} is the heat of vaporization.

The second mechanism for laser ablation is explosive boiling, much of the theoretical foundation on explosive boiling was established by Martynyuk.^{17,18} The theory of explosive boiling may be considered from either a thermodynamic or kinetic viewpoint.^{19,20} The former provides a rigorous method to predict the thermodynamic critical temperature, while the latter mechanism models the rate of formation of vapor bubble growth at any temperature. According to thermodynamic theory of explosive boiling, the liquid begins to be superheated and becomes metastable when it exceeds a temperature of about $0.80T_{\text{tc}}$. When the laser irradiance is high enough (10^9 W/cm² or above), the temperature of the target heated by the laser pulse can exceed $0.80T_{\text{tc}}$, as a result, a superheated metastable liquid layer forms. Homogeneous bubble nucleation will occur in this superheated layer, and the “liquid” is essentially a mixture of liquid droplets and vapor that can facilitate explosive boiling.

It is reasonable to suggest that mass below the irradiance threshold is removed at the surface by normal vaporization, while dramatic increase in ablation depth is related to the explosive boiling. However, whether explosive boiling occurs during the laser pulse or after the laser pulse has not been fully established? Miotello and Kelly⁷ argued that explosive boiling may occur during the laser pulse. However, in our case, from the experiment as well as kinetic theory of explosive boiling, we found that explosive boiling should take place after the completion of laser-material interaction. First, the experimental results show that large size particulates are ejected about 300–400 ns after laser pulse. Second, according to kinetic theory of explosive boiling, it is not an inevitable process when the liquid is superheated.²¹ Homogeneous bubble nucleation occurs when the liquid is superheated, but only if these bubbles have enough time to reach a critical radius r_c , will they grow spontaneously. Then the liquid experiences large density fluctuation, and large size particulates are then ejected from the target surface. The critical radius r_c can be expressed as²²

$$r_c = \frac{2\sigma}{p_{\text{sat}}(T_l) \exp\{\nu_l [p_l - p_{\text{sat}}(T_l)] / R_v T_l\} - \rho_l}, \quad (2)$$

where σ is the surface tension of the liquid, R_v is the gas constant, and ρ_l is the densities of superheated liquid/vapor with $\nu_l = 1/\rho_l$. T_l is the temperature of the superheated liquid, which can be taken as $0.85T_{\text{tc}}$ when explosive boiling occurs. Using the method suggested by Martynyuk,¹⁸ we estimated that the thermodynamic critical temperature of silicon is ap-

proximately 5200 K. p_{sat} is the saturation pressure at the superheated liquid temperature, which can be obtained from the Clausius–Clayperon relation. p_l is the pressure of the superheated liquid, and it can be approximated by the recoil pressure of the evaporating vapor, which is $0.54p_{\text{sat}}(T_l)$.²³ According to the power law relation of surface tension σ for liquid metal, the surface tension drops about 80% at the assumed T_l .²⁴ This relation is also satisfied for silicon as liquid silicon behaves much like a liquid metal.²⁴ Using these parameters, we estimate r_c to be approximately 0.6 μm . However, the thermal penetration depth during a laser pulse of duration τ is $x_{\text{th}}=0.969[(k\tau)^{1/2}]$,²⁵ (k is the thermal diffusivity of the liquid silicon, which is about 0.75 cm^2/s), which in our case is about 0.47 μm for 3 ns laser pulse. The critical diameter of the bubble is $d_c=2r_c$, or 1.2 μm , which is larger than the thermal penetration depth; the bubble cannot grow to its critical radius during the laser pulse. Experimental evidence suggests that explosive boiling occurs only if the superheated layer is thick enough.¹⁹ Even if the explosive boiling occurs, the ablation depth is approximately equal to the thermal penetration depth, which is about 0.47 μm . However, in our experiment the maximum ablation depth is about 22 μm . Therefore, explosive boiling should occur after the laser pulse when the superheated layer is sufficiently thick.

In the superheated liquid, bubble growth is strongly influenced by the momentum interaction between the growing bubble and the surrounding liquid being pushing away. The bubble growth in this time regime is given by²²

$$R(t) = \left\{ \frac{2}{3} \left[\frac{T_l - T_{\text{sat}}(p_l)}{T_{\text{sat}}(p_l)} \right] \frac{L_{\text{ev}} \rho_v}{\rho_l} \right\}^{\frac{1}{2}} t \quad (3)$$

ρ_v is the densities of superheated liquid/vapor, T_{sat} is saturation temperature of the superheated liquid pressure, which can be obtained from the Clausius–Clayperon relation. τ_c is the time for vapor bubble to grow from initiation (of very small radii, several mean atomic spacings) to the critical radius r_c . It can be calculated by letting left side of Eq. (3) equal r_c , and we can calculate that τ_c is about 70 ns. It indicates that the bubble will take about 70 ns to grow to the critical radius of 0.6 μm , then the superheated liquid transforms into a mixture of vapor and liquid droplets, followed by explosive boiling. However, our laser pulse duration is only 3 ns, from Eq. (3), the bubble radius can only grow up to about 0.025 μm in 3 ns. As a result, without efficient energy dissipation, the liquid temperature can exceed the critical temperature if the laser irradiance is sufficiently high. Therefore, it is unlikely that explosive boiling will occur during laser pulse. A high temperature region will be formed near the surface, which will eventually penetrates into the target. The bubbles will reach the critical radius after a time of τ_c ; in experiments, micron-sized droplet ejection occurred 300–400 ns after the completion of the laser pulse. Violent ejection of particulates lasts for several microseconds; For this period of time, we can estimate the thermal penetration depth is on the order of 10 μm , which is consistent with the experimental ablation depth for laser irradiance above the threshold.

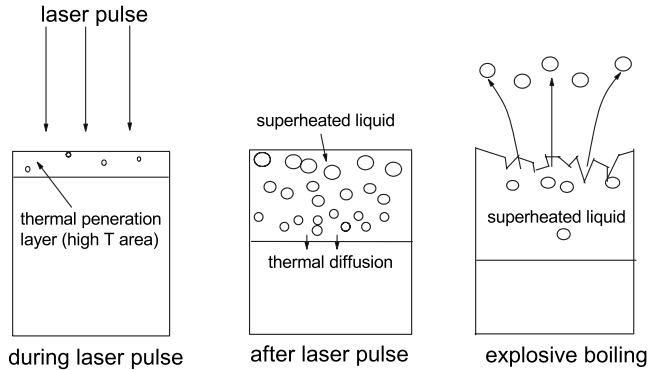


FIG. 2. The processes of laser ablation—explosive boiling.

From the kinetic theory, we can also calculate the rate of homogeneous nucleation by²⁶

$$I_n \approx 1.5 \times 10^{32} \exp(-\Delta G_n/k_B T) \exp(-\tau_{\text{hn}}/t) \text{ nuclei/cm}^3 \text{ s} \quad (4)$$

Here ΔG_n is the free energy for the formation of a stable homogeneous nucleus. τ_{hn} is the relevant time constant, which ranges from 1 to 100 ns according to Martynuk,²⁷ and as the estimation of Kelly and Miotello²⁸ it is about 30 ns. I_n is numerically significant (i.e., $I_n \geq 1$) only when the temperature is near to T_{tc} . As an example, the value for Cs is $I_n=1 \text{ nucleus/cm}^3 \text{ s}$ at $T=0.874T_{\text{tc}}$ and $I_n=10^{26} \text{ nuclei/cm}^3 \text{ s}$ at $T=0.905T_{\text{tc}}$. The number of homogeneous nuclei which would be generated during the laser pulse is $I_n V^* \tau$, where V^* is the heated volume during the laser pulse, and $V^*=\frac{1}{4}\pi x_{\text{th}} D_{\text{laser}}^2$. D_{laser} is the width of the laser pulse (in our experiments, 35 μm), so $V^* \approx 4.5 \times 10^{-10} \text{ cm}^3$. Take $I_n=10^{26} \text{ nuclei/cm}^3$ and $\tau_{\text{hn}}=50 \text{ ns}$, the homogeneous nuclei generated during the laser pulse equals 5. For such a low generation ration of nuclei, explosive boiling cannot be expected to occur during laser pulse.

From the above analysis, very few vapor bubble can be generated near the surface of the target during the laser pulse. Even if the bubbles are formed, they do not have enough time to grow up to the critical radius, thus explosive boiling will not occur. Therefore, little energy provided by the laser pulse can be dissipated, and a high temperature layer will be formed at and below the target surface during the laser pulse with a depth approximately equal to the thermal penetration depth. At the same time the target undergoes normal vaporization from the extreme outer surface, and an expanding plasma will form due to the interaction of laser pulse with the vapor. As a consequence, a portion of the laser energy will be shielded by the plasma. Mass ablation below the laser irradiance threshold is dominated by this normal vaporization mechanism. The vaporization flux is governed by Eq. (1). At high laser irradiance, after the laser pulse is completed, the high temperature liquid layer will propagate into the target with thermal diffusion. New bubbles will emerge in the superheated liquid, after the thickness of the superheated layer is larger than the critical diameter, the bubbles will grow spontaneously inside it. This superheated layer will eventually leave the target. This process is described in Fig. 2. Consistent with experiments, large particu-

lates are ejected from the target several hundred nanoseconds after laser pulse.

IV. NUMERICAL SIMULATIONS

A numerical model based on this diffusion-phase explosion mechanism has been established to determine the depth of the superheated layer. The computed depths are used as an indication of the liquid layer that is indicative to explosive boiling. To solve the time-dependent temperature distribution in the sample, the following conservation of energy equation for laser heating is used:

$$\rho C \frac{\partial T}{\partial t} = \frac{\partial}{\partial x} \left(k \frac{\partial T}{\partial x} \right) + \alpha I_{\text{laser}} \exp(-\alpha x). \quad (5)$$

where T is the temperature, C is the specific heat, and I_{laser} is the laser irradiance that reaches the surface of the silicon target. The spatial coordinate x is in the direction normal to the sample surface with the origin located at the surface.

For solving Eq. (5), boundary conditions are required at $x=0$ and $x=L$, where L is the length of the computational domain. At $x=L$, the temperature of the material is assumed to be unaffected by the laser irradiation, i.e., $T(L, t > 0) = T_0$, T_0 is the initial temperature of the solid. For $x=0$, energy loss to the surrounding air can be ignored because the heat flux is negligible compared to the latent heat of the evaporating vapor. Thus, an adiabatic boundary condition, i.e., $\partial T / \partial x = 0$, was used when there is no surface evaporation. When vaporization exists at the surface, the energy loss was calculated as the latent heat of evaporating mass. The energy reaching the surface of the target I_{laser} , is then equal to the difference between the incident laser energy and the latent heat of evaporation at the surface,

$$I_{\text{laser}} = (1 - R)I(0, t) - L_{\text{ev}}\rho_l v, \quad (6)$$

where v is the receding velocity of the sample surface during evaporation, R is the reflectivity of laser energy at the target surface, and $I(0, t)$ is the laser irradiance at the surface of the target.

We use a Gaussian energy distribution as the laser pulse source. The spatial domain of 60 or 120 μm (depending on the wavelength of the laser) was uniformly divided with grid size of 15 nm. The time step is 1 ps. The initial temperature of the sample is 300 K. The thermal and optical properties of silicon for different laser wavelengths have been published in literature.^{29–34}

We include in the model the absorption of laser-generated plasma from the target surface. Such a plasma is frequently observed during high power laser ablation of solids. However, it has previously not been included for modeling laser ablation in the explosive boiling regime. The laser-induced plasma above the surface can shield a portion of the laser beam during the pulse, here we only consider the loss of laser energy due to the collision by electrons with atoms and ions (inverse Bremsstrahlung process).^{34,35} In this model, the ablated vapor is described by three components: electrons, ions, and neutral atoms with subscripts e , i , and α , respectively.

The energy of electrons is^{35–37}

$$\varepsilon = \frac{3}{2}n_e k_B T_e + n_e k_B \theta_i. \quad (7)$$

The first term is the kinetic energy and the second is ionization energy. T_e and n_e are electron temperature and density. θ_i is the ionization potential, which is about 94 584 K. The first term is kinetic energy and the second is ionization energy. The energy of particles is

$$\varepsilon_p = \frac{3}{2}n_p k_B T_p, \quad (8)$$

where T_p and n_p are particle temperature and density, respectively. Here, particles include ions and neutral atoms, so the particle density can be expressed as

$$n_p = n_i + n_\alpha, \quad (9)$$

where n_i and n_α are the ion and atom densities, respectively. We assume that the electron density is equal to the ion density, i.e., $n_e = n_i$.

The change in electron energy equals energy absorbed from the laser pulse minus energy transferred to particles via collision. Assuming that the density and temperature are homogeneous in the entire vapor cloud, the energy equation of electrons can be written as

$$\frac{d\varepsilon_e}{dt} = \frac{[1 - \exp(-Hk_1)]}{H}(1 - R_0)I_0(t) - \frac{3}{2}k_B(T_e - T_p)v_{\text{tr}}n_e, \quad (10)$$

where $I_0(t)$ is the laser intensity as a function of time, v_{tr} is the energy transfer frequency, k_1 is the absorption coefficient of the plasma, H is the thickness of plasma, and R_0 is the reflectivity of the target. The reflectivity decreases to zero during the laser pulse after surface melting start, so here we choose $R_0=0$. The plume is assumed to expand with sonic velocity,

$$\frac{dH}{dt} = \sqrt{\frac{\gamma k_B T_p}{M}},$$

where γ is the ratio of C_p and C_v , and M is particle mass. The absorption coefficient for inverse Bremsstrahlung is defined as³⁷

$$k_1 = \frac{3.7 \times 10^8}{\omega^3 \sqrt{T_e}} \left[\exp\left(\frac{h\omega}{k_B T_e}\right) - 1 \right] n_e n_i + \frac{e^2 v_e n_e}{\pi m c \omega}, \quad (11)$$

where ω is the laser frequency, m is the electron mass, e is the electron charge, and c is the light speed. v_c is the electron-atom collision frequency,

$$v_c = n_\alpha \sigma_c \sqrt{\frac{8k_B T_e}{\pi m}}, \quad (12)$$

where σ_c is the electron-atom collision cross section.

The change in particle energy is equal to energy carried by the atom vapor ejected from the sample surface plus the energy transferred from electron via collision,

$$\frac{d\varepsilon_p}{dt} = \frac{3}{2} k_B T_s \frac{J_v}{H} + \frac{3}{2} k_B (T_e - T_p) v_{tr} n_e, \quad (13)$$

where T_s is the surface temperature of the sample.

The ionization rate is³⁷

$$\frac{dn_e}{dt} = \alpha_i n_\alpha n_e - \beta_R n_i n_e^2, \quad (14)$$

where $\alpha_i = C_i \sqrt{k_B T_e} \exp(-\theta_i/T_e)$ and $\beta_R = C_i [2(2\pi m/h)^{3/2} (g_i/g_k) k_B T_e]$. C_i is an experimental parameter determined from electron ionization cross section data. The details of the calculations of the parameters v_{tr} , α_i , and β_R can be found in Ref. 37.

The change in the density of atoms in the plasma is equal to atoms evaporated from the surface

$$\frac{d[H(n_\alpha + n_i)]}{dt} = J_v, \quad (15)$$

where J_v is the evaporation rate, which can be calculated by multiplying evaporation flux and number density of atom in the liquid.

The laser irradiance transmits through plasma and reaching the target surface I_{laser} can be written as

$$I(0,t) = I_0(t) \exp(-Hk_1). \quad (16)$$

The ablation depth by evaporation was calculated by integrating Eq. (4). During the laser pulse, a high temperature layer is formed at and beneath the surface of the target; this layer then propagates into the target by thermal diffusion. We consider the liquid whose temperature is larger than $0.80T_{lc}$ as superheated liquid, and in such a metastable state, homogeneous bubble nucleation will occur, if the thickness of the superheated layer is large enough ($\sim 4.0 \mu\text{m}$ according to experiments). Ablation for irradiance below the threshold is governed by normal evaporation according to Eq. (4). Ablation for the irradiance larger than the threshold is governed by both normal evaporation and explosive boiling.

The ablation depths predicted by this model are compared to experimental data in Fig. 1. The theoretical calculations for all three wavelengths are consistent with experiments. The model predicts that the laser irradiance threshold for explosive boiling is about 3×10^{10} and $1.5 \times 10^{11} \text{ W/cm}^2$ for 266 and 532 nm wavelengths, respectively, in good agreement with experimental values ($\sim 2 \times 10^{10}$ and $\sim 4 \times 10^{11} \text{ W/cm}^2$ for 266 and 532 nm wavelengths, respectively). In our model, the superheated liquid reaches its maximum depth of 100–1000 ns after the laser pulse is completed, which also agrees with experimental results. For 1064 nm wavelength laser ablation of silicon, from theoretical calculation, explosive boiling also does not occur.

The temperature distribution at different times is described in Fig. 3. For 266 and 532 nm wavelengths, the laser irradiances are chosen at their thresholds of explosive boiling, which are 3×10^{10} and $1.5 \times 10^{11} \text{ W/cm}^2$, respectively. For 1064 nm wavelength, the irradiance for maximum ablation depth is used. A high temperature layer is formed during the laser pulse. After the laser pulse, the high temperature layer penetrates into the target, and the surface temperature is not the highest due to evaporation at the surface. For 266 nm

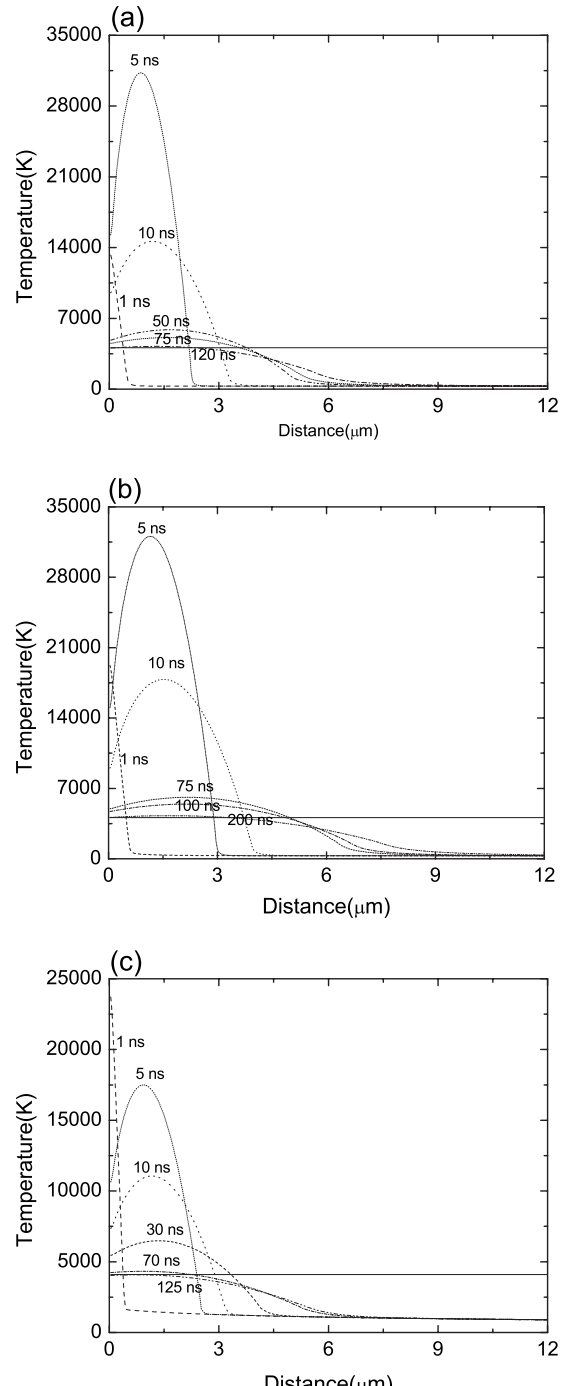


FIG. 3. The temperature distribution at different times. (a) 266 nm wavelength, laser irradiance of $I=3 \times 10^{10} \text{ W/cm}^2$. (b) 532 nm wavelength, laser irradiance of $I=1.5 \times 10^{11} \text{ W/cm}^2$. (c) 1064 nm wavelength, laser irradiance of $I=4.0 \times 10^{11} \text{ W/cm}^2$. (The layer above the solid line is superheated layer).

laser pulse, the superheated layer reaches its maximum thickness about $4.0 \mu\text{m}$ at 75 ns. For 532 nm wavelength, the superheated layer has a maximum thickness of $4.5 \mu\text{m}$ at 100 ns. For 1064 nm, it reaches a maximum superheated layer at 30 ns, with a thickness of $3.2 \mu\text{m}$, then it reduces gradually, at 125 ns the superheated layer vanishes, this can explain why explosive boiling does not occur.

Plasma shielding plays an important role in determining the laser irradiance threshold for explosive boiling. The effect of plasma shielding can be illustrated by plotting the

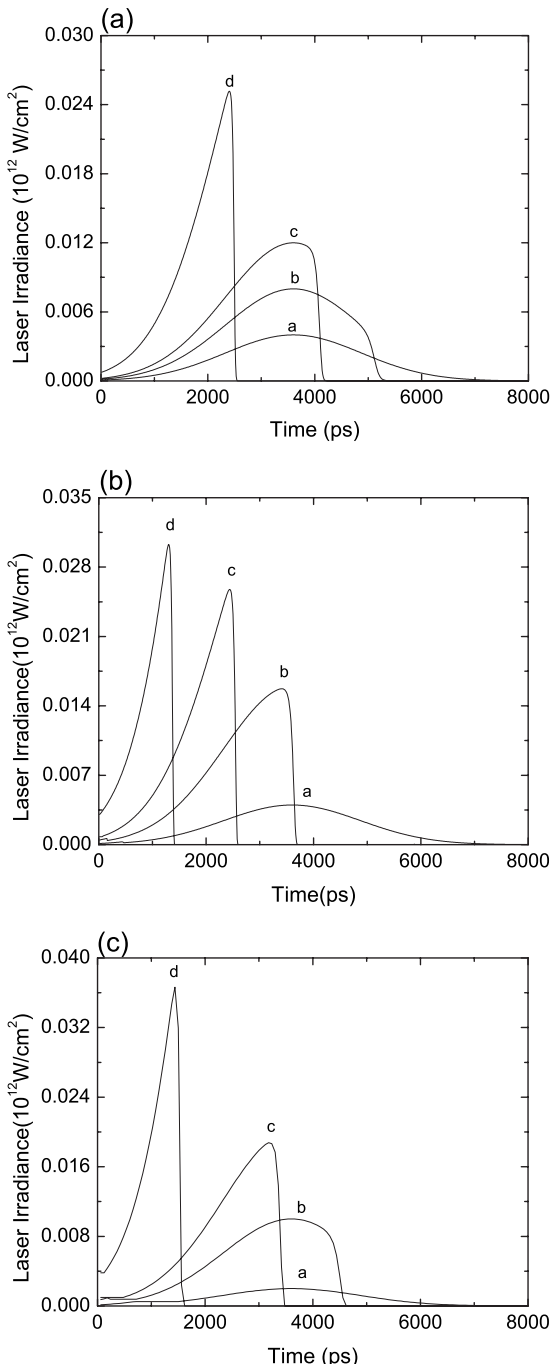


FIG. 4. Temporal profiles of laser irradiance on the target surface for different initial peak laser irradiances, I_{peak} , before the interaction with a mass plasma. (a) 266 nm wavelength, the values of I_{peak} are a: 10^{10} , b: 2×10^{10} , c: 3×10^{10} , and d: $1 \times 10^{11} \text{ W/cm}^2$. (b) 532 nm wavelength, the values of I_{peak} are a: 10^{10} , b: 4×10^{10} , c: 1.5×10^{11} , and d: $4 \times 10^{11} \text{ W/cm}^2$. (c) 1064 nm wavelength, the values of I_{peak} are a: 10^{10} , b: 5×10^{10} , c: 1×10^{11} , and d: $8 \times 10^{10} \text{ W/cm}^2$.

transmitted laser temporal profile through the plasma (Fig. 4). When the laser irradiance is low, the laser pulse retains its original profile with little attenuation by the plasma. However, when the laser irradiance is large, the trailing part of the laser pulse is truncated. The larger the laser irradiance, the more the laser energy is truncated.

V. CONCLUSIONS

As measured from experiments, for 266 and 532 nm wavelength laser ablations of silicon, there exists a laser ir-

radiance threshold that corresponds to a dramatic increase in the ablation depth. Below the threshold, the ablation depth increases slowly. However, at the threshold, the ablation depth increases dramatically, which accompanies large particulates ejected 300–400 ns after the completion of ablation laser pulse. We developed a theoretical analysis for this threshold phenomenon, which includes the effect of plasma shielding. We conclude that the mass is removed by normal evaporation for laser irradiance below the threshold. For laser irradiance above the threshold, during the laser pulse the mass is removed by normal evaporation. At the same time, a plasma forms due to the interaction of laser pulse with the vapor, which shields part of the laser energy. A high temperature layer near the surface of the target is formed during the laser pulse, which penetrates into the target after the completion of laser interaction. When the superheated is thick enough, explosive boiling occurs. Plasma shielding during laser irradiation was found to have a significant effect on the threshold phenomenon, and our calculations provide a satisfactory estimate of the experimental results. Although our experiment and our model are based on 3 ns laser pulse interaction with silicon, it should be applicable for a broad range of pulse durations according to the analysis that is not material specific.

ACKNOWLEDGMENTS

This research has been supported by the Chemical Science Division, Office of Basic Energy Sciences, U.S. Department of Energy, under Contract No. DE-AC02-05CH11231, and the U.S. Department of Defense, Army Research Office, MURI program. Q. M. Lu was also supported by the National Science Foundation of China under Grant No. 40725013.

- ¹S. S. Mao, F. Quéré, S. Guizard, X. Mao, R. E. Russo, G. Petite, and P. Martin, *Appl. Phys. A: Mater. Sci. Process.* **79**, 1695 (2004).
- ²R. E. Russo, X. Mao, and S. S. Mao, *Anal. Chem.* **74**, 70A (2002).
- ³*Laser Ablation and Deposition*, edited by J. C. Miller and R. F. Haglund (Academic, New York, 1998).
- ⁴R. F. Wood, C. W. White, and R. T. Young, *Pulsed Laser Processing of Semiconductors* (Academic, Orlando, 1984).
- ⁵M. D. Levenson, E. Mazur, P. S. Pershan, and Y. R. Shen, *Resonance* (World Scientific, Singapore, 1990).
- ⁶A. Okano and K. Takayanagi, *J. Appl. Phys.* **86**, 3964 (1999).
- ⁷A. Miotello and R. Kelly, *Appl. Phys. Lett.* **67**, 3535 (1995).
- ⁸R. Kelly and A. Miotello, *J. Appl. Phys.* **87**, 3177 (2000).
- ⁹J. H. Yoo, S. H. Jeong, R. Greif, and R. E. Russo, *J. Appl. Phys.* **88**, 1638 (2000).
- ¹⁰J. H. Yoo, S. H. Jeong, X. L. Mao, R. Grief, and R. E. Russo, *Appl. Phys. Lett.* **76**, 783 (2000).
- ¹¹Q. M. Lu, S. S. Mao, X. Mao, and R. E. Russo, *Appl. Phys. Lett.* **80**, 3072 (2002).
- ¹²L. J. Radziemski and D. A. Cremers, *Laser-Induced Plasmas and Application* (Dekker, New York, 1989).
- ¹³J. R. Ho, C. P. Grigoropoulos, and J. A. Humphrey, *J. Appl. Phys.* **79**, 7205 (1996).
- ¹⁴L. Balazs, R. Gijbels, and A. Vertes, *Anal. Chem.* **63**, 314 (1991).
- ¹⁵A. Peterlongo, A. Miotello, and R. Kelly, *Phys. Rev. E* **50**, 4716 (1994).
- ¹⁶G. M. Pound, *J. Phys. Chem. Ref. Data* **1**, 135 (1972).
- ¹⁷M. M. Martynyuk, *Sov. Phys. Tech. Phys.* **19**, 793 (1974).
- ¹⁸M. M. Martynyuk, *Russ. J. Phys. Chem.* **57**, 494 (1983).
- ¹⁹R. C. Reid, *Am. Sci.* **64**, 146 (1976).
- ²⁰Q. M. Lu, *Phys. Rev. E* **67**, 016410 (2003).
- ²¹J. U. Seydel and W. Fucke, *J. Phys. F: Met. Phys.* **8**, L157 (1978).
- ²²V. P. Carey, *Liquid-Vapor Phase Phenomena* (Hemisphere, Washington,

1992).

²³M. Von Allmen, *Laser Beam Interactions with Materials* (Springer, Heidelberg, 1987).

²⁴A. Yoshida, J. Jpn. Inst. Met. **58**, 1161 (1994).

²⁵C. R. Phipps, T. P. Turner, R. F. Harrison, G. W. York, W. Z. Osborne, G. K. Anderson, X. F. Corlis, L. C. Haynes, H. S. Steels, and K. C. Spicochi, *J. Appl. Phys.* **64**, 1083 (1988).

²⁶M. M. Martynyuk, Sov. Phys. Tech. Phys. **21**, 430 (1976).

²⁷M. M. Martynyuk, Radio Eng. Electron. Phys. **25**, 100 (1980).

²⁸R. Kelly and A. Miotello, *Phys. Rev. E* **60**, 2616 (1999).

²⁹S. de Unamuno and E. Fogarassy, *Appl. Surf. Sci.* **36**, 1 (1989).

³⁰R. O. Bell, M. Toulemonde, and P. Siffert, *Appl. Phys.* **19**, 313 (1979).

³¹I. Lukes, R. Sasik, and R. Cerny, *Appl. Phys. A* **54**, 327 (1992).

³²O. Muller, S. de Unamuno, B. Prevot, and P. Dhamelincourt, *Phys. Status Solidi A* **158**, 385 (1996).

³³H. A. Weakliem and D. Redfield, *J. Appl. Phys.* **50**, 1491 (1979).

³⁴G. E. Jellison, Jr. and F. A. Modine, *Appl. Phys. Lett.* **41**, 180 (1982).

³⁵X. L. Mao and R. E. Russo, *Appl. Phys. A* **64**, 539 (1997).

³⁶I. Ursu, I. N. Mihaescu, I. Apostol, M. Dinescu, A. Hening, M. Stoica, A. M. Prokhorov, V. P. Ageev, V. I. Konov, and V. N. Tokarev, *J. Phys. D* **17**, 1315 (1984).

³⁷R. J. Harrach, "Theory for laser-induced breakdown over a vaporizing target surface," Lawrence Livermore Laboratory, University of California Report No. UCRL-52389, 1987.